Electronic Properties of Catechol Adsorbed on Rutile TiO 2 and SnO 2 (110) Surfaces: A Density Functional Theory Study

Article · January 2016

CITATIONS
0

READS
311

9 authors, including:

George Amolo
The Technical University of Kenya
50 PUBLICATIONS **220** CITATIONS
SEE PROFILE

N.W. Makau
University of Eldoret
27 PUBLICATIONS **181** CITATIONS
SEE PROFILE

Samuel Lutta
University of Eldoret
25 PUBLICATIONS **510** CITATIONS
SEE PROFILE

Julius Mwakondo Mwabora
University of Nairobi
51 PUBLICATIONS **973** CITATIONS
SEE PROFILE

Electronic Properties of Catechol Adsorbed on Rutile TiO_2 and SnO_2 (110) Surfaces: A Density Functional Theory Study

Victor Meng'wa[1,*], George Amolo[1], Nicholas Makau[1], Samuel Lutta[2], Maurice Okoth[2]
Julius Mwabora[3], Robinson Musembi[3], Christopher Maghanga[4] and Robert Gateru[5]
[1] *Computational Materials Science Group, Department of Physics, University of Eldoret, Eldoret, Kenya*
[2] *Department of Chemistry and Biochemistry, University of Eldoret, Eldoret, Kenya*
[3] *Department of Physics, University of Nairobi, Nairobi, Kenya*
[4] *Department of Physics, Kabarak University, Kabarak, Kenya*
[5] *Kenya Methodist University, Nairobi, Kenya*

The incorporation of organic molecules such as catechol onto TiO_2 substrate to enhance TiO_2 photocatalytic activity has led to improved Dye Sensitized Solar Cells (DSSCs) efficiency. Nonetheless, it still remains low for most practical applications hence more detailed description of the electronic structure of catechol-TiO_2 rutile surface, could provide insight for further improvement. In this work, adsorption of catechol on rutile TiO_2 and SnO_2 (110) surfaces has been studied using first principle methods. The study investigated the role played by catechol in varying the electronic structure of TiO_2 and SnO_2 (110) surfaces. Results obtained showed that both the clean and catechol-terminated stoichiometric (110) TiO_2 four layer surface had a band gap of 2.1 eV. The energy gap increased by 0.32 eV which represents an 18 % increment from 1.7 eV for clean stoichiometric TiO_2 to 2.02 eV following adsorption of catechol molecule on the TiO_2 (110) rutile 5-layer surface. The highest occupied molecular orbital (HOMO) in the four and five layered catechol terminated TiO_2 (110) surfaces was found to be about 1 eV, above the valence band maximum edge but in SnO_2 it nearly overlapped with bottom of conduction band. The lowest unoccupied molecular orbital (LUMO) in both TiO_2 and SnO_2 surfaces was located about 3 eV above the conduction band minimum, while the band gap of the molecule was in the range of 4.0 eV. The presence of catechol related C-2p orbitals within the energy gap and conduction band suggests that the energy level alignment of catechol adsorbed onto TiO_2 suits the electron transfer processes that occur in DSSCs. The overlap of fermi level and closeness of catechol's HOMO to conduction band minimum in catechol bound (110) rutile SnO_2 surface shows that the surface may become conductive and hence, inappropriate for photocatalytic applications.

1. Introduction

Titanium dioxide (TiO_2) has attracted a lot of interest due to its potential applications in various fields such as catalysis, photoelectrode in DSSCs, gas sensor, white pigment in paints and cosmetics as well as electric devices such as varistors [1]. The application of TiO_2 as a semiconductor in the dye sensitized solar cells (DSSCs) has made this cell affordable and a promising source of renewable energy. Pure TiO_2 is a wide band gap semiconductor, with its optical absorption being limited to the ultra-violet range. Several approaches have been proposed to lower the absorption threshold to the more usable visible region [2-4]. In this regard, chromopheres-sensitized TiO_2 have attracted a lot of attention and extensive study which has led to a remarkable improvement of DSSCs efficiency, although more efforts are still needed to make dye/TiO_2 perfomance better in DSSCs. Chromopheres used in the DSSCs are expected to bind to TiO_2, match the semiconductor energy levels and be photochemically and thermally stable [5]. Use of nanostructured TiO_2 thin films has led to increased solar energy conversion efficiency of DSSCs to about 10% [6], although efforts are still ongoing to improve on this even further.

Catechol molecule ($C_6H_2O_2$) is a small organic dye sensitizer that is photoactive and binds to semiconductor photocatalysts by OH groups. Its often used as an anchoring group for larger more complex organic and inorganic dyes and forms type II heterojunctions [7].

Curtiss et al. [8] studied catechol-TiO_2 anatase system using different sizes of hydrogen-terminated cluster models, where they established that large clusters gave more reliable results. Dick and Ralph [9] performed TDDFT computations on dye sensitized TiO_2 nanowires and observed that catechol sensitization on TiO_2 nanowire shifts the absorption spectrum to visible range hence more photoabsorption and attributed this mainly to local interactions between the

*victormengwa@gmail.com

dye and the TiO_2 nanowire and not linked to the periodic nature of the system.

Ramamoorthy and Vanderbilt [10] calculated the total energy of periodic TiO_2 slabs using self-consistent *ab initio* method, where it was shown that the (110) surface has the lowest surface energy, while (001) surface has the highest. Indeed, it has been shown that a rutile TiO_2 crystal is dominated by the (110) planes which makes it attractive to study the dye-semiconductor interface for the (110) surfaces. It has been reported that surface modification of nanocrystalline TiO_2 particles with different catechol-type derivatives alters the optical properties [11].

Among the three polymorphs of TiO_2, the anatase phase has been extensively studied for possible applications in DSSCs [11-14]. On the other hand, rutile TiO_2, which is more chemically stable and cheap to grow has received little attention in DSSCs applications regardless of the fact that it has superior light-scattering properties due to its higher refractive index [16].

T. Bredow, et al. [17] studied the oscillations in geometric and electronic properties of thin rutile TiO_2 (110) films as a function of the number of layers in the films. They showed that the strong oscillations are an intrinsic property of thin rutile TiO_2 films and that they are largely connected to the presence of an even or odd number of layers in the film. The main reason for the oscillations is the change in O (2p) - Ti(3d) interlayer hybridization along the film. They further noted that these oscillations, determine both the geometric and the electronic structure of the rutile TiO_2 films. This makes the study of catechol-sensitized TiO_2 rutile (110) surface on odd and even layer quite relevant because electronic properties are critical in photocalytic applications.

Although many materials have been proposed as possible alternatives for TiO_2, SnO_2 is the most promising option which is used as an electrode in DSSCs. Addition of Al_2O_3, makes it even more viable as an electrode for DSSCs, because the conduction band-edge for SnO_2 is less negative than that of TiO_2. Incorporation of SnO_2 as a semiconductor in DSSC makes it possible to be used with far red-absorbing chromophores having excited states too low in energy to inject into TiO_2.

In this work, we present electronic structure calculations of catechol terminated rutile TiO_2 and SnO_2 (110) surfaces with 4-layer (even) and 5-layer (odd) slabs. The band structure, projected density of states and relative positions of catecholate HOMO and LUMO have been determined. The effects of the even (4) and odd (5) layers on electronic properties catechol-TiO_2 (110) surface have been discussed.

2. Computational Methodology

All the calculations reported in this work were performed within the density functional theory [18] using the generalized gradient approximation [19] as implemented in the Quantum Espresso code [20]. Ultrasoft PW91-pseudopotentials were used to model core-valence interactions for O, Ti and Sn atoms. Plane waves with kinetic-energy cutoff of 30 Ry were used for expanding the Kohn-Sham wave functions for both O, Ti and Sn. Full optimization of the cell parameters (a and c) for the bulk rutile TiO_2 and SnO_2 were carried out and their values are reported in the shown table. The truncated TiO_2 and SnO_2 (110) rutile slabs were built from the calculated equilibrium bulk structures.

TABLE 1: Calculated DFT-GGA lattice parameters (Å) of bulk rutile TiO_2 and SnO_2 and their respective experimental values [1,21].

	Parameters	This Work	Experimental
TiO_2	a	4.59	4.58
	c	2.96	2.95
SnO_2	a	4.74	4.74
	c	3.19	3.19

Electronic and structural calculations were carried out using Davidson algorithm with total energy accuracy of 10^{-6} and 10^{-7} Ry for catechol-bound and clean slabs, respectively. The Monkhorst-Pack mesh was used to sample the irreducible part of Brillouin zone [22]. A k-point mesh of $4 \times 4 \times 1$ was used for clean surfaces and $2 \times 2 \times 1$ for the catechol bound-TiO_2 and SnO_2. A thick vacuum layer ($\backsim$ 20 Å thickness) was included in the direction perpendicular to the surface to avoid interaction between periodic images. The catechol molecule was adsorbed perpendicularly on one side of the slab only. The oxygen atoms from catechol were anchored on the undersaturated Ti_{5C} site of the TiO_2 (110) surface and the undersaturated Sn_{5C} atom of SnO_2 (110) surface which resulted to two Ti-O and Sn-O bonds, respectively (see Figs. 4 and 7). As a result, the bridging oxygen atoms (O_{2C}) on TiO_2 and SnO_2 surfaces terminated with hydrogen atoms split from the catechol molecule to form OH groups on SnO_2 and TiO_2 surfaces.

3. Results and Discussions

3.1. Structure of the relaxed rutile 4-layer (4L) and 5-layer (5L) (110) TiO_2 surface

A stoichiometric (110) TiO_2 rutile surface normally has a reduced coordination of titanium and oxygen atoms as shown in Fig. 1. The surface contains sixfold coordinated (Ti_{6C}) atoms just like in the bulk and fivefold coordinated (Ti_{5C}) atoms that are missing one bond. Two different kinds of oxygen atoms are also created; threefold coordinated oxygen atoms (O_{3C}) as in the bulk which lie on the main surface plane, while twofold coordinated oxygen atoms (O_{2C}) also known as bridging oxygen atoms miss one bond as a result of the missing layer. A stoichiometric SnO_2 (110) surface has a similar structure as shown in Fig. 1, the Ti atoms are replaced with Sn atoms.

The clean relaxed 4L and 5L (110) TiO_2 surfaces are shown in Figs. 2 and 3, where the bond lengths of the surface and sub-surface atoms are indicated. After relaxation, the bond lengths between the sixfold coordinated (Ti_{6C}) and twofold coordinated (O_{2C}) surface atoms contracted by an average of 0.06% in relation to bulk bonds while those between sixfold coordinated (Ti_{6C}) and threefold coordinated (O_{3C}) expanded by 2.28%. Bond lengths connected to the surface fivefold coordinated (Ti_{5C}) atoms and sub-surface three fold coordinated (O_{3C}) atoms reduced by 8% which indicates a significant inward relaxation towards the bulk. The surface atoms were found to relax towards the vacuum

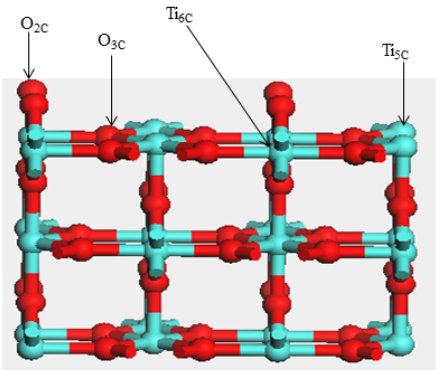

FIG. 1: Bulk truncated rutile TiO_2 (110) surface showing surface atom coordination

except the Ti_{5C} atom that relaxed towards the bulk. The relaxation of surface atoms in the z-direction (towards the vacuum) ranged between 0.1 Å and 0.3 Å but no significant relaxation of these atoms was observed in x and y directions. As such, the surface was slightly buckled.

An important observation between the clean 4L and 5L surfaces is that there were different structural rearrangements occurring in the TiO_2 surfaces as a function of the number of layers. In particular, the 4L surface showed a significant increase of about 19 % in the separation between the second and third layers, while a small increment of between 1.4 % and 8 % was noted in the 5L surface, an observation that was in agreement with other workers [17].

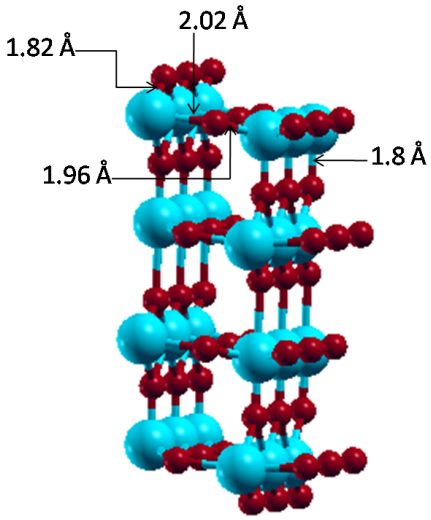

FIG. 2: Relaxed 4L-clean TiO_2 (110) surface.The red (small) and light blue spheres (large) represent O and Ti atoms, respectively

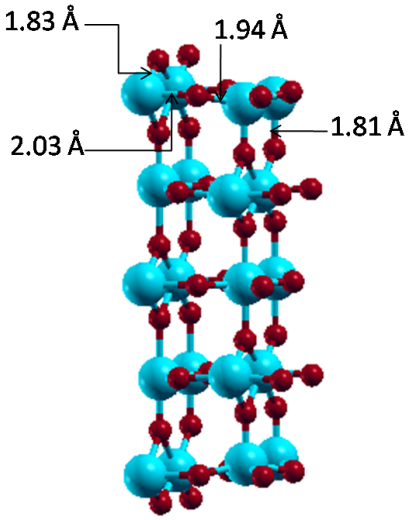

FIG. 3: Relaxed 5L-clean TiO_2 (110) surface. The spheres represent the atoms as described in FIG. 2 above

3.2. Adsorption Geometry of Dissociated catechol on (110) rutile TiO_2 Surface

Fig. 4 shows the relaxed 4L structure of catechol-terminated TiO_2 (110) rutile surface, where the molecule adsorbs in an upright configuration with the benzene ring being perpendicular to the surface. The adsorption modes of catechol molecule on 4L-TiO_2 and 5L-TiO_2 (110) surface are shown in Figs. 4 and 5. These patterns are simplified in Fig. 6 (a) and (b), where they are known as bindate mononuclear chelating and bindate binuclear chelating, similar to what was reported by Jankovic et al. [15]. This may have occured due to the varying size of the adsorption surface plane where the 5L-TiO_2 was 2 × 2 and the 4L-TiO_2 was 3 × 2 in symmetry.

The presence of catechol resulted in the distance between the second and third layers that lie in the middle of relaxed 4L-TiO_2 surface to increase by 0.31 Å, thereby weakening further the interaction between these layers. Furthermore, the interface bond lengths between oxygen atoms of the catechol molecule and Ti_{5C} atoms were separated by 2.12 Å, which represents an increase of 0.55 Å compared to a similar bond in the unrelaxed catechol-TiO_2 structure. The hydrogen atoms split from catechol, formed O-H bonds with O atoms from TiO_2 and these were slightly tilted after relaxation from their vertical positions on the 4L-TiO_2 surface plane.

Unlike in the 4L case, the catechol molecule adsorbed on the 5L-structure (see Fig. 5) was tilted away from the vertical direction and a significant displacement of the Ti_{5C} atom was observed so as to accommodate the bonding of both catechol oxygen atoms. For the 5L-TiO_2/catechol structure (see Fig. 5), the relaxed Ti-O bond length between oxygen atoms from the catechol molecule and the Ti_{5C} surface atom was found to be about 2.1 Å, which represents an increase of 5 % compared to the same bond for the structure before relaxation. The Ti_{5C} atoms in the relaxed surface, buckled outwards by 0.83 Å above the TiO_2

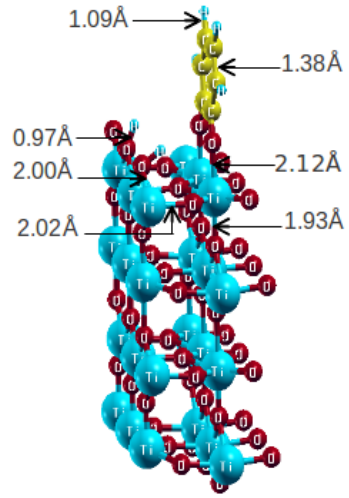

FIG. 4: Relaxed 4L-TiO_2 (110) surface with anchored catechol molecule. Note that the molecule is perpendicular to the surface

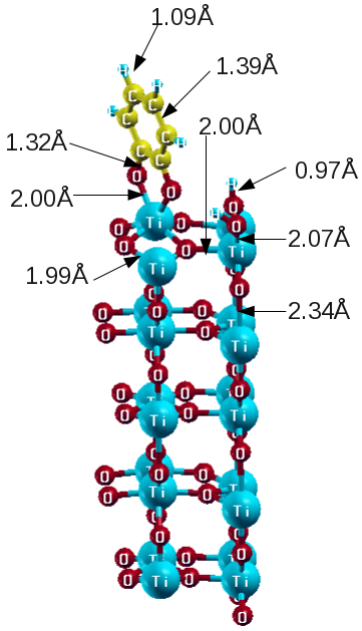

FIG. 5: Relaxed 5L-TiO_2 (110) surface with anchored catechol molecule. Note that the molecule is tilted slightly from the perpendicular axis

surface level as a result of bonding to the oxygen atoms of the catechol molecule. Sub surface Ti and O atoms also moved from their bulk positions by about 0.16 Å in the +z-direction following the adsorption of the catechol molecule. The dissociated hydrogen atoms from catechol were found to bond with the bridging oxygen atoms and these were found to be displaced towards the TiO_2 surface plane by small distances ranging from 0.04 Å to 0.40 Å and slightly

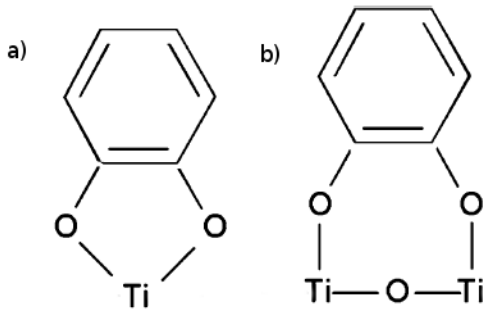

FIG. 6: a) bindate mononuclear chelating and b) bindate binuclear chelating

tilted from their vertical positions. The Ti-O bond length for the sub surface atoms was found to be elongated by a range of 0.36 to 0.99 Å as a result of catechol adsorption.

3.3. Adsorption Geometry of Dissociated catechol on (110) rutile SnO_2 Surfaces

Catechol molecule was adsorbed onto the 5L-SnO_2 (110) surface but upon relaxation, it tilted away from vertical position as shown in Fig. 7, reproducing a similar pattern to that of catechol/5L-TiO_2 system shown in Fig. 5. The bond length between oxygen atoms of the molecule and Sn_{5C} atom was 2.18 Å, which is an increase of 20 % compared to Sn-O bond lengths on a clean rutile SnO_2 (110) surface. Adsorption of catechol therefore causes a significant amount of displacement of the surface and sub-surface atoms. In particular, the Sn_{5C} atom that is bonded to the catechol oxygen atoms moved upwards by 0.89 Å from its position on the clean surface. The dissociated hydrogen atoms from catechol bonded to both bridging oxygen atoms (O_{2C}) shifted downwards by between 0.3 Å and 0.5 Å compared to their unrelaxed atomic positions. These atoms also experienced angular displacement of 5.8 and 20.66 degrees away from their vertical positions, respectively, in order to accommodate steric hindrance and other surface effects (see Fig. 7). The bridging oxygen atoms (O_b) did not change their positions significantly. The sub surface atoms of SnO_2 and TiO_2 surfaces moved by smaller amounts of between 0.04 Å to 0.08 Å due to the presence of the catechol molecule.

For the 4L-SnO_2/catechol surface shown in Fig. 8, there was no pronounced displacement of Sn_{5C} surface atoms. The atomic displacements remained almost the same as in 5L-SnO_2/catechol relaxed surface. The adsorption pattern of catechol on the 4L-SnO_2 surface is similar to that of the 4L-TiO_2/catechol system, except the bond between two Sn_{5C} atoms and catechol's oxygen atoms which was slightly inclined by 7 degrees from the perpendicular position on 4L-SnO_2/catechol surface compared to the orientation of catechol on 4L-TiO_2 surface.

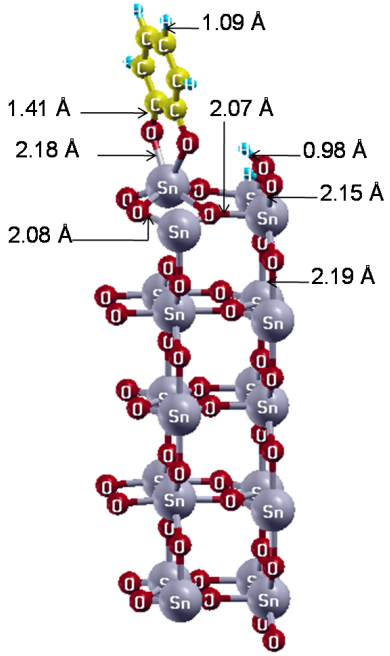

FIG. 7: Relaxed 5L-SnO_2 (110) surface with anchored catechol molecule

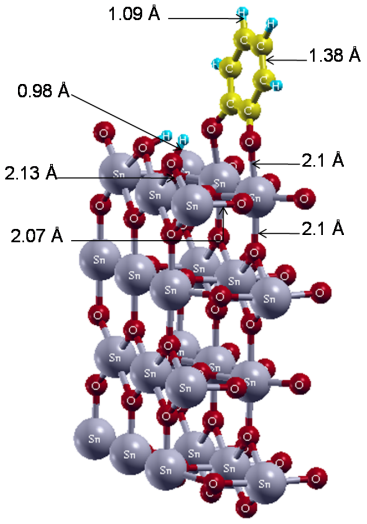

FIG. 8: Relaxed 4L-SnO_2 (110) surface with anchored catechol molecule

3.4. Electronic structure of 4L and 5L stoichiometric TiO_2 (110) clean rutile surface

Figs. 9 and 10 shows the electronic band structure (BS) and projected density of states (PDOS) of clean even (4L) and odd (5L) TiO_2 (110) surfaces.

From the band structure plots, 4L and 5L TiO_2 (110) surfaces have direct energy gaps of 2.1 eV and 1.7 eV, respectively, at Γ, that are underestimated in comparison to the theoretical values obtained by calculations with CRYSTAL06 program quoted at 3.24 eV [23]. This difference in the bandgap values is mainly attributed to the use of hybrid density functional methods employed in the CRYSTAL06 program, which utilises atomic basis sets and hybrid pseudopotentials [24]. The Fermi energy level is clearly shown with a label E_f in the BS and PDOS figures. The features of 5L and 4L TiO_2 slabs are similar except for the narrower energy band gap of 1.7 eV for 5L-TiO_2 slab.This is attributed to the shifting of the position of the bottom of the conduction band, while the top of the valence band remains the same (see Fig. 9).The bottom of the conduction band is mainly composed of Ti-3d orbitals (see Fig. 10), hence the observed band gap variation as a function of the number of layers is largely dependent on the contribution from Ti-3d orbitals. This suggests that the surface truncation has a role to play with regard to the final surface properties and near-surface structure and hence the final application of the TiO_2 surfaces.

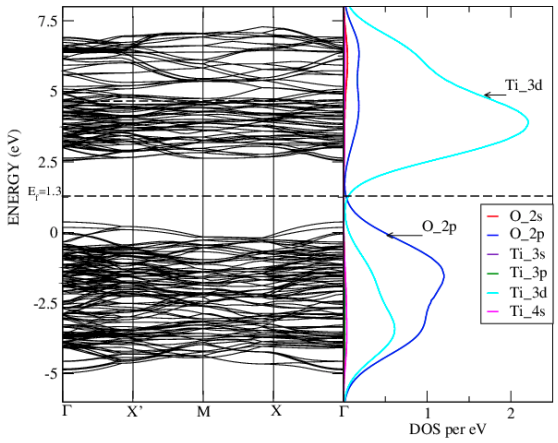

FIG. 9: Band structure (BS) and projected density of states (PDOS) of clean 4L-TiO_2 (110) rutile surface

The higher binding energies, not shown here are populated by O-2s core states. The upper valence band from -5 eV to almost 0.37 eV is mainly dominated by O-2p states, with some considerable contribution from Ti-3d states which are responsible for Ti-O bonding. The conduction band consists mainly of unoccupied Ti-3d and O-2p states. No states were observed in the energy gap of the clean rutile TiO_2 (110) surface, confirming that the clean TiO_2 surface is indeed an insulator.

3.5. Electronic structure of 4L-TiO_2 rutile (110) surface with adsorbed catechol molecule

The Projected density of states (PDOS) and band structure of stoichiometric (110) TiO_2 4L- slab with catechol adsorbate are shown in Fig. 11.

Upon adsorption of catechol on the (110) TiO_2 rutile surface, new mid gap states were found to occur within the energy gap, in particular, a C-2p peak is located around 2.5 eV. We regarded this as the HOMO of the catechol molecule.

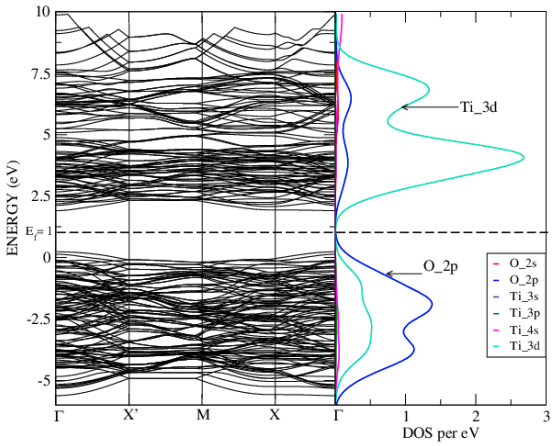

FIG. 10: BS and PDOS of 5L-TiO_2 rutile clean (110) surface

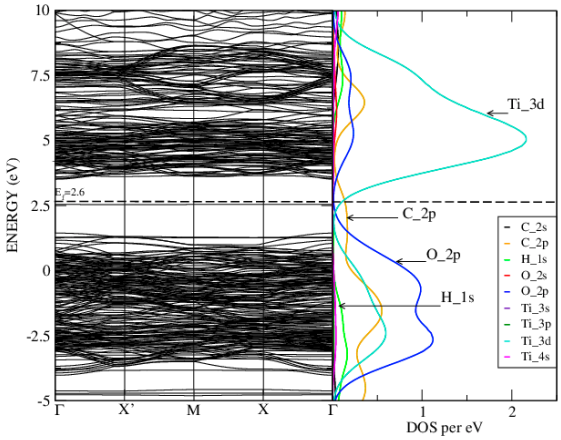

FIG. 11: BS and PDOS of 4L-TiO_2 (110) surface with catechol termination

The isosurface density of the midgap state shown in Fig. 12 clearly indicates the state is from catechol adsorbate. In the conduction band, catechol related C-2p states were

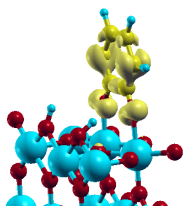

FIG. 12: Isodensity surface of midgap state in BS and PDOS of catechol/4L-TiO_2 (110) surface

more pronounced at 3 eV above the CB edge. This constitutes the LUMO of the catechol molecule. Thus, the difference between catechol's LUMO (about 6.5 eV) and HOMO (about 2.5 eV) energies provides an estimate of the energy gap of the molecule found to be about 4 eV. Despite its low intramolecular excitation of 300 nm (∼4 eV), catechol adsorption on TiO_2 shifts the optical absorption threshold to 420 nm (2.98 eV) which facilitates visible light absorption [25]. The upper valence band is dominated by O-2p and C-2p states with significant contribution from Ti-3d orbitals. This hybridization confirms the observed strong bonding between the TiO_2 surface and the catechol molecule. In the conduction band, the Ti-3d states were found to be the most predominant with a mixture of O-2p and C-2p states. As a consequence of hybridization of the C-2p orbital with Ti-3d orbitals, optical transition between these midgap states and conduction band would produce charge transfer similar to transition from VB to CB of bulk TiO_2.

The hydrogenated bridging oxygen atoms (O_{2C}) orbital coupling may not have contributed to states within the energy gap but it may have stabilized the catechol/metal oxide systems by making the bonds not to dangle. It is further noted that in the 4L-slab, the band gap remained as 2.1 eV at Γ, hence not affected by the molecular adsorbate. The energy gap of 2.1 eV is lower compared to catechol modified-TiO_2 energy gaps estimated by UV-vis spectroscopy and other DFT calculations of 2.4 eV and 2.48 eV [26], respectively. It is well known [27] that simple DFT-based approaches fail to predict the energy gaps accurately due to errors inherent to the functionals used in the local density and the generalized gradient approximations. These errors are significantly reduced by post-DFT methods like DFT+U and hybrid functionals [26]. The shift in the absorption threshold indicates that interactions of catechol with the TiO_2 surface exhibit visible-light absorption which originate from electronic transitions between surface Ti-OH group of catechol. Furthermore, incooperation of catechol into the band structure of the clean 4L-TiO_2 (110) surface has no effect on the size of the energy gap.

3.6. Electronic structure of 5L-TiO_2 (110) surface with adsorbed catechol molecule

The projected density of states plotted alongside the band structure for the fully relaxed catechol/5L-TiO_2 (110) system are shown in figure 13. Just as in the case of the catechol/4L-TiO_2 surface, the HOMO in the catechol/5L-TiO_2 is located within the semiconductor band gap, about 1 eV above the VB edge and localized on the catechol molecule. Additionally, the isosurface density of the midgap state in the catechol/5L-TiO_2 is similar to the one shown in Fig. 12 and is derived from catechol adsorbate. The LUMO is centred exclusively in the conduction band of the TiO_2 substrate and is found at 3 eV above the CB edge. The qualitative shape of the PDOS and, most importantly, the relative positions of HOMO, LUMO, VB and CB edges remain unaltered compared to the clean TiO_2 surface. The DFT calculated energy gap was slightly modified by the presence of catechol molecule to 2.02 eV. This represents an energy gap increase of 0.32 eV, which is 18 % increase, from 1.7 eV of clean 5L TiO_2 (110) surface. The observed change in the energy gap is attributed to the adsorption of the catechol molecule on the TiO_2 substrate, suggesting that adsorption of catechol on rutile (110) surface has a significant effect on the electronic properties of the 5-layered rutile slab. Specifically the energy gap of the 4L-TiO_2 slab

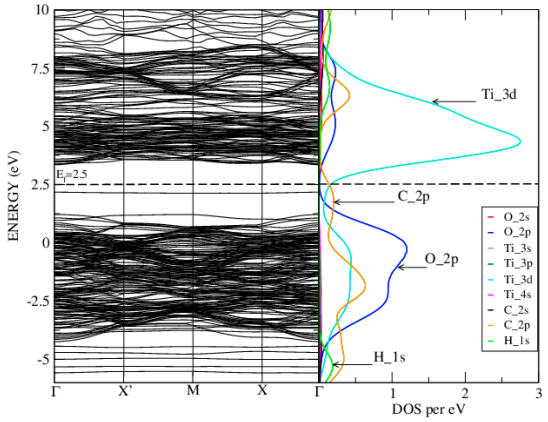

FIG. 13: BS and PDOS of 5L-TiO_2 (110) stoichiometric surface with catechol adsorbate

with and without adsorbate remained 2.1 eV at Γ, whereas for the 5L-TiO_2 slab it increased by 0.32 eV. This change in the electronic properties is attributed to a shift in the position of the CBM of the 5L slab as observed in (Fig. 13). This can easily be deduced by the observed shift in the position of E_f, where an E_f increase of 50 % more is seen for 5L-TiO_2/catechol when compared to similar increase for 4L-TiO_2/catechol.

3.7. Electronic structure of 4L and 5L stoichiometric (110) SnO_2 rutile surface with adsorbed catechol molecule

Plots of the band structure and PDOS of clean and catechol bound 4L stoichiometric rutile SnO_2 (110) surfaces are shown in Figs. 14 and 15, respectively. The electronic structures of clean and catechol bonded 4L and 5L SnO_2 (110) surfaces are similar hence the BS and PDOS of 5L-SnO_2 slabs are not shown here.

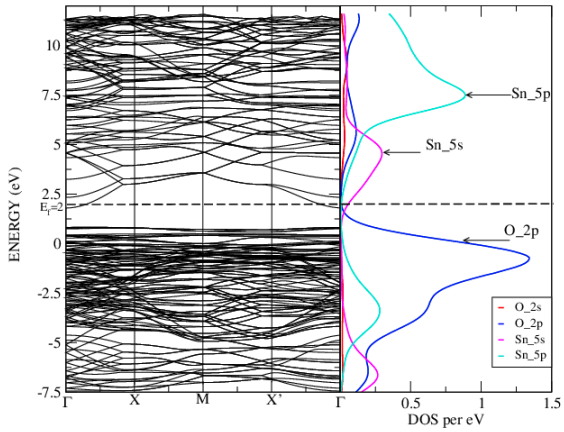

FIG. 14: BS and PDOS of clean 4L SnO_2 (110) surfaces

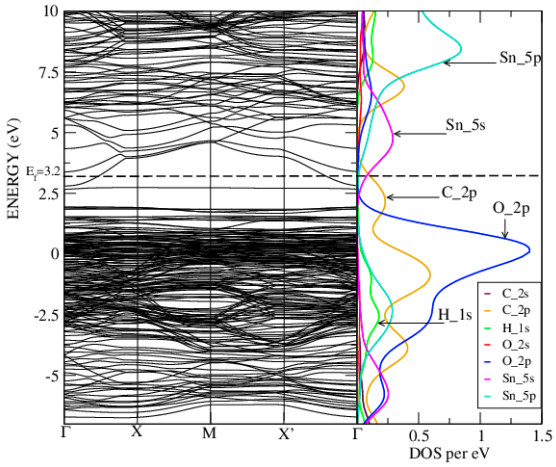

FIG. 15: BS and PDOS of 4L stoichiometric (110) SnO_2 surface with catechol adsorbate

Both Figs. 14 and 15 show energy gaps that are drastically reduced in relation to a previous theoretical calculation that found a band gap of 2.68 eV [21] for clean (110) SnO_2 surface. Other than, the usual underestimation of the energy gaps by DFT due to their exchange-correlation formulation, adsorption of catechol (see Fig. 14) increased the number of the states located in the conduction band minimum, which makes them shift downwards, thereby narrowing the energy gap. This downwards band bending implies an increase in conductivity. However, the energy gap of 5L-TiO_2 that has catechol adsorbed on it, showed an increase when compared to that of the corresponding clean (110) rutile 5L-TiO_2. Therefore, catechol appears to act differently in modifying the size of the energy gaps of SnO_2 and TiO_2. This significantly affects their DSSC applications. It is observed that the states within the energy gap of SnO_2 (110) surface with adsorbed catechol, overlap with the bottom of the conduction band, thereby increasing conductivity. Moreover, the states at the top of the valence band are almost flat, unlike the bottom of the conduction band whose states were curved and dispersed. This dispersed band also contributes to the lowering of optical absorption due to interconduction transition, which makes SnO_2 a good transparent conductor [28].

The conduction band minimum was dominated by Sn 5s orbitals (see Figs. 14 and 15), which have also been noticed from other calculations to contribute partially to the reduction of the bandgap [29]. The upper valence band is largely occupied by O 2p states, whereas the contribution of C 2p and Sn 5p states is moderate, thereby increasing hybridization. Within the energy gap region, C 2p states from the catechol adsorbate are seen. The upper conduction band (CB) contained a significant contribution from Sn 5p orbitals and moderate contribution from C 2p. Sn 5s states were predominant in the lower part of the CB.

The HOMO of the catechol adsorbate was clearly visible above the valence band maximum, being centered at 2.5 eV and it overlaped with the CB minimum. In the CB, a prominent feature that was attributed to the catechol adsorbate was recognizable at 6.5 eV as C 2p peak. The calculated energy is given by the energy difference between 2.5

eV (HOMO) for the occupied states and 6.5 eV (LUMO) for the unoccupied states giving a gap value of 4 eV for the catechol molecule. Due to the overlap of the states as a result of catechol molecule, the stoichiometric rutile SnO_2 (110) surface is conductive.

Consequences of catechol-modified electronic structure of TiO_2 and SnO_2 (110) rutile surfaces for DSSCs Application

Our discussions reveal that catechol/TiO_2 is a better photocatalyst than catechol/SnO_2. In the catechol-sensitized TiO_2, the location of catechol molecule C-2p state within the TiO_2 energy gap, which constitutes the molecular HOMO and the more pronounced molecular peak that forms the LUMO well inside the TiO_2 conduction band, shows clearly an energy level alignment necessary for the functioning of a DSSCs. In the DSSCs, the dye is in contact with TiO_2 film and upon irradiation of the dye, an excited electron is injected from the dye to TiO_2 conduction band, which then proceeds to the cell anode. Furthermore, such surface modification of TiO_2 by catechol extends the absorption range of TiO_2 from UV region to the visible range. This is consistent with studies of Dick and Ralph [9] of absorption spectra of catechol adsorbed on TiO_2 anatase nanowire which showed photoabsorption in the optical region above 400 nm. As a result of the shift, more photogenerated electrons and holes will be available to participate in the photocatalytic reaction since 95% of solar light reaching the ground is visible light. Subsequently, this will make the DSSCs more effective and efficient.

4. Conclusion

The structural and electronic properties of 4-layer and 5-layer TiO_2 (110) surfaces terminated with catechol molecule have been determined. The surface atoms were observed to relax towards the vacuum (z-direction) except for the five-fold coordinated Ti_{5C} atom. Relaxations in the x and y directions were negligible. The projected density of states showed that the conduction band derived states mainly from Ti-3d orbitals, while the top of valence band is a hybridization of O-2p and Ti-3d states.

The catechol molecule was anchored onto both 4L and 5L SnO_2 and TiO_2 (110) surfaces by bindate binuclear chelating for 4L-slabs and bindate mononuclear chelating for 5L-slabs. The presence of catechol adsorbate did not alter significantly the electronic structure of catechol sensitized SnO_2 and TiO_2 (110) surfaces when compared to clean SnO_2 and TiO_2 (110) surfaces. However, the alignment of catecholate orbitals which occured in the energy gap (HOMO) and within the conduction band (LUMO) were in agreement with the expected coupling of dye/TiO_2 electronic structure for DSSC's applications. Our calculations approximated well the catechol's HOMO- LUMO gap of 4 eV.

From catechol-terminated TiO_2 (110) slabs, there is significant contribution of C-2p orbitals from catechol adsorbate in VB, CB and within the band gap. The band gap of the 4L-TiO_2 slab remained unaltered with and without the adsorbate while the band gap of the 5L-TiO_2 surface increased by 0.32 eV. Based on our DFT results, the 4L-TiO_2 slab offers better estimation of the energy gap than the 5L-TiO_2 slab. Thus, its not only the orientation of the surface that plays a key role in the desired surface structure properties, but also the surface truncation (surface bonds) is important.

The 4L-slabs with wider surface planes adsorbed catechol in an upright configuration while for 5L-slabs with small surface planes, the adsorbed catechol was slightly tilted from vertical orientation. Surface modification of TiO_2 by catechol enhances TiO_2 photocatalytic activity necessary for energy applications such as in DSSCs and promotes the understanding of the electronic effects at the organic dye/TiO_2 interface, which are useful knowledge in designing more suitable photocatalysts with better performance.

Unlike TiO_2, catechol adsorption onto SnO_2, narrowed the energy gap, and hence making SnO_2 to behave as a conductor. Such an energy gap leads to lower voltages in the DSSC, hence SnO_2 would serve better as an electrode in the DSSC rather than a semiconductor.

Acknowledgements

Computational resources were provided by Centre for High Performance Computing (CHPC). This joint collaborative work was supported by the National Commission for Science, Technology and Innovation (NACOSTI), Kenya Government, through a grant, NCST/5/003/4TH CALL/050. The authors are most grateful.

References

[1] U. Diebold, Surf. Sci. Rep. **48**, 53 (2003).
[2] J. Moser, S. Punchihewa, P. P. Infelta and M. Gratzel, Langmuir **7**, 3012 (1991).
[3] T. Rajh, J. M. Nedeljkovic, L. X. Chen, O. Poluektov and M. C. Thurnauer, J. Phys. Chem. B **103**, 3515 (1999).
[4] E. Vrachnou, N. Vlachopoulos and M. Gratzel, Chem. Comm. 868 (1987).
[5] R. Argazzi, N. Iha, H. Zabri, F. Odobel and C. Bignozzi, Coord. Chem. Rev. **248**, 1299 (2004).
[6] L. Gundlach, R. Ernstorfer and F. Willig. J. Phys. Rev. B **74**, 035324 (2006).
[7] A. Calzolari, A. Ruini and A. Catellani, J. Am. Chem. Soc. **133**, 58935899 (2011).
[8] L. A. Curtiss, P. C. Redfern, P. Zapol, T. Rajh and M. C. Thurnauer, J. Phys. Chem. B. **107**, 11419 (2003).
[9] D. Douma and R. Gebauer, Phys. Status Solidi RRL **5**, No.8, 259 (2011).
[10] M. Ramamoorthy and D. Vanderbilt, Phys. Rev. B **49**, 16721 (1994).
[11] I. A. Jankoviċ, Z. V. Šaponjiċ, M. I. Čomor and J. M. Nedeljkoviċ, J. Phys. Chem. C **113**, 12645 (2009).
[12] M. Law, L. Greene, J. Johnson, R. Saykally and P. Yang, Nat. Mater. **4**, 455459 (2005).
[13] H. Kusama, M. Kurashige, K. Sayama, M. Yanagida and H. Sugihara, J. Photochem. Photobiol. A **189**, 100104 (2007).

[14] J. Wu, S. Hao, J. Lin, M. Huang, Y. Huang, Z. Lan and P. Li, Cryst. Growth Des. **8**, 247252 (2008).
[15] W. R. Duncan and O. V. Prezhdo, Phys. Chem. B **58**, 143 (2007).
[16] K. Kim, K. Benkstein, J. van de Lagemaat and A. Frank, Chem. Mater. **14**, 10421047 (2002).
[17] T. Bredow, L. Giordano, F. Cinquini and G. Pacchioni. J. Phys. Rev. **70**, 035419 (2004).
[18] P. Hohenberg and W. Kohn. J. Phys. Rev. **136** (3B), B864 (1964).
[19] J. Perdew, K. Burke and M. Ernzerhof, Phys. Rev. Lett. **80** No.4, 891 (1998).
[20] P. Giannozzi et al., J. Phys.: Condensed Matter **21**, 395502 (2009).
[21] M. Batzill and U. Diebold. Progress in Surf. Sci. **79**, 47154 (2005).
[22] H. Monkhorst and J. D. Pack. Phys. Rev. B **13** (12), 5188 (1976).
[23] A. Beltran, J. Andres, J. Sambrano and E. Longo, J. Phys. Chem. A **112**, Issue 38 (2008).
[24] R. Dovesi, V. Saunders, C. Roetti, R. Orlando, M. Zicovichwilson, F. Pascale, B. Civalleri, K. Doll, N. Harrison, J. Bush and Ph. Llunnel, CRYSTAL06 User's Manual (University of Torino, 2006).
[25] P. Persson, R. Bergstrom and S. Lunnel, J. Phys. Chem. B **104**, 10348 (2000).
[26] S. Higashimoto, T. Nishi, M. Yasukawa, M. Azuma, Y. Sakata and H. Kobayashi, J. Catalysis **329**, 286 (2015).
[27] C. Di Valentin, G. Pacchioni and A. Selloni, Phys. Rev. Lett. **97**, 166803 (2006).
[28] M. A. Maki-Jaskari, T. Rantala and V. Golovanov, Surf. Sci. **577**, 127 (2005).
[29] K. Reimann and M. Steube, Solid State Commun. **105**, 649 (1998).

Received: 21 July, 2016
Accepted: 16 September, 2016